An old approach for new investigations in the IBA symmetry triangle

E.A. McCutchan
WNSL, Yale University, New Haven, Connecticut 06520-8124, U.S.A.

Recibido el 1 de febrero de 2006; aceptado el 30 de marzo de 2006

Motivated by the success of the X(5) critical point model in describing the properties of certain rare-earth nuclei, IBA-1 calculations are performed for rare-earth isotopic chains. Contours of basic observables are discussed and used to extract parameter values. The properties of all low-lying positive parity excitations are well described for a wide range of nuclei and the resulting parameters are mapped into the IBA symmetry triangle. The simple, two parameter IBA-1 calculations are also extended to the Pt isotopic chain. Both energies and electromagnetic transition strengths are are found to be well described over the entire isotopic chain suggesting these nuclei can be described more simply without the need for introducing an intruder configuration.

Keywords: Interacting boson model; collective levels; B(E2) values.

Motivado por el éxito del modelo del punto crítico X(5) se hicieron cálculos en el modelo de bosones interactuantes IBA-1 para cadenas de núcleos en la región de las tierras raras. Se discuten contornos de observables básicos para determinar los coeficientes de las interacciones. Se encuentra una buena descripción de todos los estados excitados a bajas energías en una gran variedad de núcleos. Se hace un mapeo de los parámetros del modelo al triángulo de simetría. Se discute una extensión de este cálculo sencillo con nada más dos parámetros a los isótopos de Pt. El buen ajuste encontrado para las energías y las transiciones electromagnéticas sugiere que no es necesario introducir configuraciones intrusas para describir las propiedades de estos núcleos.

Descriptores: Modelo de bosones interactuantes; excitaciones colectivas, valores B(E2).

PACS: 21.10.Re; 21.60.Fw; 27.70.+q

1. Introduction

The introduction of the critical point symmetry X(5) [1], which describes nuclei at the critical point of the transition from spherical to axially symmetric deformed shapes, has resulted in an increased focus on the properties of excited 0^+ states. Along with specific predictions for the yrast band structure, a key component of the X(5) model is the prediction for the energy of the first excited 0^+ state. Experimentally, an X(5)-like structure has been observed in several rare-earth nuclei (see for example Ref. 2 to 5). The ability of the X(5) model to describe these nuclei is remarkable considering that the model is parameter free (except for scale).

The rare-earth nuclei provide an interesting region to investigate on a broader scale the evolution from spherical to deformed structures. An analysis of the evolution of structure across entire rare-earth isotopic chains using the interacting boson approximation (IBA) model [6] has been previously performed [7]. These calculations focused on the yrast states and the γ-band obtaining generally good agreement, however, the predictions for 0_2^+ states were mixed, deviating from the data by large amounts for the more neutron rich nuclei. The recent success of the X(5) model in describing the properties of excited 0^+ states in some rare-earth nuclei prompted the present investigation into this region to determine sets of IBA parameters which reproduce the properties of all low-lying positive parity excitations, including the first excited 0^+ state.

2. Contours in the IBA triangle

The three dynamical symmetries of the IBA as well as structures intermediate between the three limits can be described with the extended consistent Q formalism (ECQF) [8] with the Hamiltonian

$$H = \epsilon n_d - \kappa \hat{Q}^\chi \cdot \hat{Q}^\chi \tag{1}$$

where

$$\hat{Q}^\chi = (s^\dagger \tilde{d} + d^\dagger s) + \chi (d^\dagger \tilde{d})^{(2)} \tag{2}$$

and $\hat{n}_d = d^\dagger \tilde{d}$. In this formalism, the same quadrupole operator is used in the Hamiltonian and the $E2$ operator. The Hamiltonian of Eq. (1) involves three parameters, ϵ, κ, and χ. Since the competition between the spherical and deformed terms in the above Hamiltonian is an essential component (given by the ratio of ϵ/κ), a further simplification of the ECQF Hamiltonian can be obtained by introducing a single new parameter, ζ, given by $\zeta = 4N_B/(\epsilon/\kappa + 4N_B)$. The ECQF Hamiltonian can then be rewritten as [9, 10]

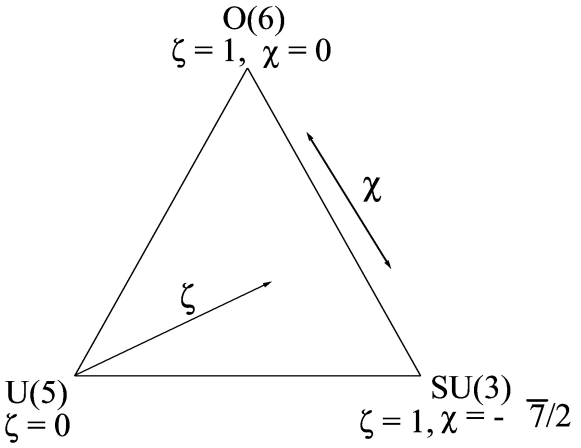

FIGURE 1. The IBA symmetry triangle. Symmetry limits are given in terms of the parameterization of Eq. (3).

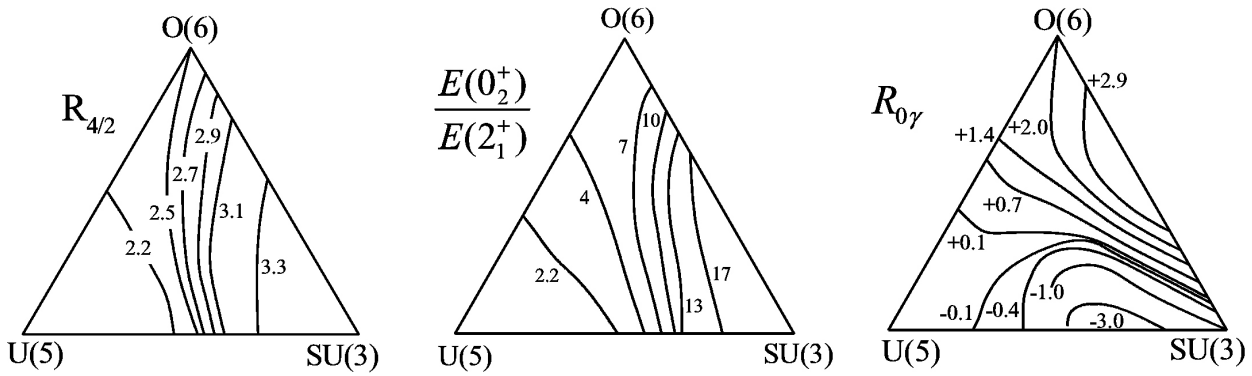

FIGURE 2. Contours of constant values of the $R_{4/2}$ energy ratio (left), the $E(0_2^+)/E(2_1^+)$ energy ratio (middle) and the $R_{0\gamma}$ ratio (right). Calculations are for N_B = 10.

$$H(\zeta) = c\left[(1-\zeta)\hat{n}_d - \frac{\zeta}{4N_B}\hat{Q}^\chi \cdot \hat{Q}^\chi\right] \qquad (3)$$

The Hamiltonian of Eq. (3) involves two parameters, ζ and χ (c is a scaling factor). The boson number N_B is given by half the number of valence protons and neutrons, each taken separately relative to the nearest closed shell.

The parameter space for this Hamiltonian is conveniently represented by a triangle [11] with one IBA dynamical symmetry at each vertex. Figure 1 illustrates the IBA symmetry triangle with the three dynamical symmetries in terms of the parameterization of Eq. (3). In this parameterization, the three symmetries are given by ζ = 0, any χ for U(5), ζ = 1, χ = -$\sqrt{7}$/2 for SU(3), and ζ = 1, χ = 0 for O(6). Transition regions between the three symmetries can be described by numerical diagonalizations of the above Hamiltonian for intermediate parameter values.

To quantitatively describe the IBA parameter space within the symmetry triangle, a coordinate system can be implemented. Using a simple set of polar coordinates [12], the IBA parameters ζ and χ of Eq. (3) can be converted into radial and angular coordinates (ρ, θ) by

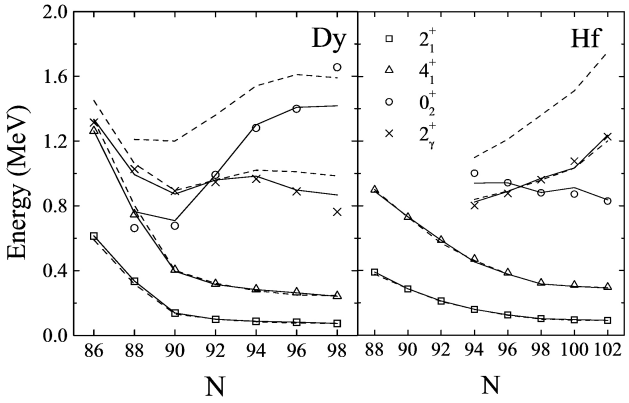

FIGURE 3. Comparison of experimental level energies (symbols) and IBA calculations of Ref. 7 (dashed lines) and the present work (solid lines) for the 2_1^+ and 4_1^+ members of the ground state band and the heads of the 2_γ^+ and 0_2^+ bands in the Dy and Hf isotopes.

$$\rho = \frac{\sqrt{3}\zeta}{\sqrt{3}\cos\theta_\chi - \sin\theta_\chi} \qquad \theta = \frac{\pi}{3} + \theta_\chi \qquad (4)$$

where $\theta_\chi = (2/\sqrt{7})\chi(\pi/3)$. These coordinates allow for a convenient and simple description of the entire triangle, with θ ranging from 0 to 60° and ρ acting as a standard radial coordinate ranging from 0 to 1.

The standard approach for determining parameter values to describe a particular nucleus is to consider contour plots of observables. In the framework of the IBA-1, this was first applied with the introduction of the consistent Q formalism [13] where contour plots of various observables as a function of N_B and χ were used to determine parameters appropriate for well-deformed nuclei. Since then, various other IBA investigations have used the same or similar contour plots, such as ϵ versus χ or ϵ/κ versus χ, to fit either individual nuclei or isotopic chains (see for example, Ref. 7, 8, and 14).

While contour plots are traditionally given in terms of the parameters of the Hamiltonian, here they will be plotted directly into the IBA triangle, using the polar coordinates of Eq. (4). This allows for a better visualization of the evolution of different observables relative to the three dynamical symmetries. The contours will also be discussed in terms of which observables are necessary to actually pinpoint the location of a nucleus in the triangle.

There are numerous experimental observables which can provide insight into nuclear structure. Here, the focus will be on the most basic observables and hence, usually the best known experimentally. For simplicity, the discussion will concentrate on the $R_{4/2} \equiv E(4_1^+)/E(2_1^+)$ energy ratio, the energy of the first excited 0^+ state and the energy of the quasi-2_γ^+ state. This approach serves only as a guide to parameter values and certainly a detailed fit to a nucleus would need to consider additional experimental observables.

Starting with the $R_{4/2}$ energy ratio, IBA calculations were performed for a mesh of ζ and χ values and parameter sets giving constant values of $R_{4/2}$ were determined. These contours can then be plotted in the IBA triangle, as given in Fig. 2 (left). The region around U(5) gives values of $R_{4/2}$ close to the vibrational limit ($R_{4/2} \sim 2.0$). With increasing ζ,

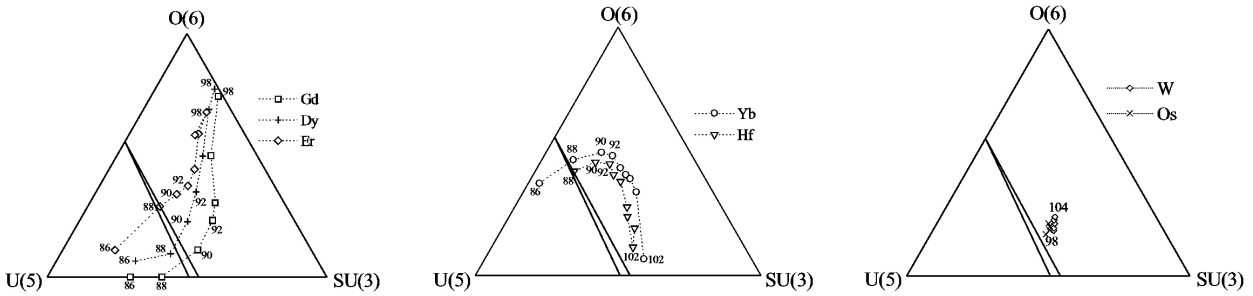

FIGURE 4. Trajectories in the IBA triangle for the Gd-Os isotopic chains. The slanting lines enclose the region of phase/shape coexistence for N_B = 10.

$R_{4/2}$ increases, approaching the axially symmetric rotational value ($R_{4/2} \sim 3.33$) in the SU(3) corner of the triangle. Clearly, the $R_{4/2}$ ratio alone does not constrain the parameter values, since each $R_{4/2}$ contour traces out a locus of parameter values in the triangle, cutting more or less vertically through the triangle.

Additional contours can be plotted in the triangle for other energy ratios, such as $E(0_2^+)/E(2_1^+)$, as shown in Fig. 2 (middle). This observable has values of 2.0 close to the U(5) region and increasing values with increasing deformation. Similar to the behavior of the $R_{4/2}$ contours, the $E(0_2^+)/E(2_1^+)$ contours trace out a somewhat vertical path through the triangle. In general, energies of individual low-lying positive parity states (normalized to the 2^+ ground state energy), such as $E(2_\gamma^+)/E(2_1^+)$, all follow a similar evolution in the IBA triangle. Overlapping these individual ratios, *e.g.*, the $E(0_2^+)/E(2_1^+)$ contours with the $R_{4/2}$ contours would not provide a unique intersection for most positions in the triangle.

To establish a unique set of parameter values for describing a nucleus requires an observable where the contours follow a more horizontal path through the triangle. Such a contour was proposed [8, 14] early on in the application of the IBA using the energy differences between different intrinsic states. A commonly used contour involves the difference between the energies of the 0_2^+ and 2_γ^+ states. A variation on this energy difference

$$R_{0\gamma} = \frac{E(0_2^+) - E(2_\gamma^+)}{E(2_1^+)} \qquad (5)$$

is plotted in the IBA triangle in Fig. 2 (right). Clearly the intersection of an $R_{4/2}$ contour with an $R_{0\gamma}$ contour would provide a unique point of parameter values for most regions of the triangle. In the following discussion, the overlap of the $R_{0\gamma}$ contours with the $R_{4/2}$ contours (along with additional observables if known experimentally) is used to extract parameter values for individual nuclei.

3. Application to rare-earth nuclei

Detailed IBA calculations were performed for collective even-even nuclei ($R_{4/2} \geq 2.0$) in the rare-earth region with Z = 64 - 76 and N = 86 - 104. In general, the energies of the low-lying positive parity excitations discussed above are described to within 5 - 10 % of the experimental values [12,15]. An example of the quality of the fits for the Dy and Hf isotopic chains is given in Fig. 3. Included in Fig. 3 are the results of the previous IBA calculations [7] for these isotopic chains. In general, the level of agreement for the ground state energies and the quasi- 2_γ^+ level is comparable in both calculations. In the present work, the agreement for the energy of the 0_2^+ state is significantly improved compared with the previous IBA calculations. The spacing the in quasi-γ band is well reproduced in most nuclei. One systematic discrepancy between the data and the calculations is in the spacing of the excited 0^+ sequence for both transitional and rotational nuclei which is expanded in the calculations compared with the experimental spacings. Additional observables, such as electromagnetic transition strengths and two neutron separation energies, are well reproduced by the present calculations.

With the identification of a set of parameters which provide a reasonable description of the evolution of the low-lying properties of states in the rare-earth nuclei, the trajectories of each isotopic chain can be quantitatively mapped into the IBA triangle. The trajectories in the symmetry triangle corresponding to the fit parameters for the Gd - Os isotopic chains are given in Fig. 4 using the polar coordinates defined in Eq. (4). With increasing neutron number, the Gd-Hf isotopic chains show an increasing quadrupole deformation, beginning near the U(5) region of the triangle, crossing the phase/shape transition region and continuing into the deformed region of the triangle. The trajectories for the W and Os isotopes lie entirely in the deformed region of the triangle. Considering the crossing of the trajectories across the phase transition region, the chains with larger Z values present an increasing γ-softness. The Gd and Dy isotopic chains cross the phase transition region close to the U(5)-SU(3) leg of the triangle whereas the Yb and Hf isotopic chains pass the phase transition region much closer to the $U(5) - O(6)$ leg of the triangle.

Past the phase transition region, the Gd, Dy and Er isotopes show an increasing γ-softness and β deformation while the Yb and Hf isotopes present an increasing γ-rigidity with almost constant β deformation. The W and Os isotopes show a slight increase in γ-softness and a rather constant β deformation. The trajectories for Gd, Dy, and Er reflect the low-

lying γ-band energy and a higher lying 0_2^+ excitation in the heavier isotopes (see Fig. 3). In contrast, the trajectories for the Yb and Hf isotopes stem from the low-lying 0_2^+ states in the heavier isotopes and the high γ-band energies. The compact, close grouping of the W and Os isotopes is a result of the near-constancy in the evolution of both the 0_2^+ and γ-band excitations.

4. Pt isotopes

The simple Hamiltonian used in the present work can describe only a limited set of nuclear shapes. The nucleus ^{188}Hg is a good example of this. ^{188}Hg has an $R_{4/2}$ value of 2.4 and an $R_{0\gamma}$ value of ~ 0. Considering the contours of Fig. 2 (left) and (right), this would place ^{188}Hg in a rather central location in the triangle. However, if the additional observable $E(0_2^+)/E(2_1^+)$ = 2.0 is considered, this can only be reproduced by a set of parameters very close to the U(5) corner of the triangle [Fig. 2 (middle)], in disagreement with the results of crossing the $R_{4/2}$ contour and the $R_{0\gamma}$ contour. The inability to describe basic observables with a consistent set of parameter values suggests additional degrees of freedom outside the space of the ECQF Hamiltonian. In the case of the Hg isotopes, it is well known [16, 17] that the additional degree of freedom involves intruder 0^+ excitations. These intruder states in Hg, as well as Pb, are explained by the promotion of two protons across the Z = 82 shell gap.

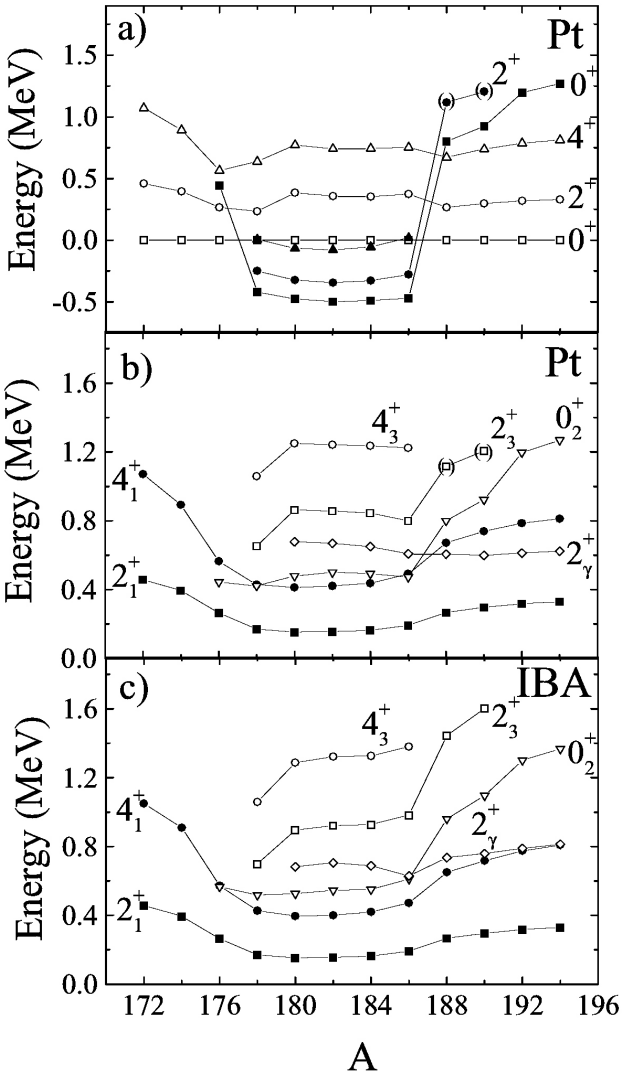

FIGURE 5. (a) Common description of the systematics of low-lying states in the Pt isotopes based on an intruder state interpretation [16, 19]. Solid (open) symbols label states interpreted as strongly (weakly) deformed. (b) Experimental level energies in the Pt isotopes where levels are connected according to their ordered appearance in energy. Solid (open) symbols label the yrast (non-yrast) states. (c) Results of the IBA calculations in the present work. Figure adopted from Ref. 20.

The concept of intruding deformed bands has been also applied to the Pt isotopes [16]. A common description of the Pt isotopes in terms of an intruder state interpretation is given in Fig. 5a. Those nuclei close to the closed neutron shell ($A \sim$ 190 - 196) are suggested to have a weakly deformed ground state (open symbols) and a more strongly deformed intruder configuration (solid symbols), lying at about 1 MeV in excitation energy. In the transition from A = 188 to A = 186, it has been proposed that the intruder configuration crosses the ground state configuration, becoming the ground state for the Pt nuclei around mid-shell. Calculations in terms of this intruder state interpretation have been performed using band mixing [18] or the IBA with configuration mixing [19]. These approaches obtain good agreement with the experimental data. However, they involve the use of numerous parameters as well as some a prior assumptions about the structure of the bands.

The connection of various states in the Pt isotopes given in Fig. 5a is therefore a model interpretation. Plotting just the excitation energies of low-lying states by their ordered appearance in energy, as in Fig. 5b, portrays quite a different picture. Considering simply the data, as given in Fig. 5b, the evolution of states is rather smooth. The yrast energies decrease as mid-shell is approached from either side. The 2_γ^+ state shows only a slight decrease in energy with increasing neutron number and the 0_2^+ state is constant in energy around mid-shell and then increases with increasing neutron number. Given the overall smooth evolution of the low-lying positive parity states, an investigation into the Pt isotopes without introducing an intruder configuration seems reasonable.

IBA-1 calculations were performed [20] for ^{172}Pt through ^{194}Pt using the methods outlined above and the Hamiltonian of Eq. (3). The results of the IBA calculations for the low-lying states are given in Fig. 5c. With a smooth evolution of parameters, the IBA can nicely reproduce the overall energy systematics observed in the Pt isotopes. Energies of the yrast band and the excited 0^+ sequence are well reproduced. The energy of the 2_γ^+ state is reproduced well for the lighter Pt isotopes and slightly overestimated for the heavier nuclei.

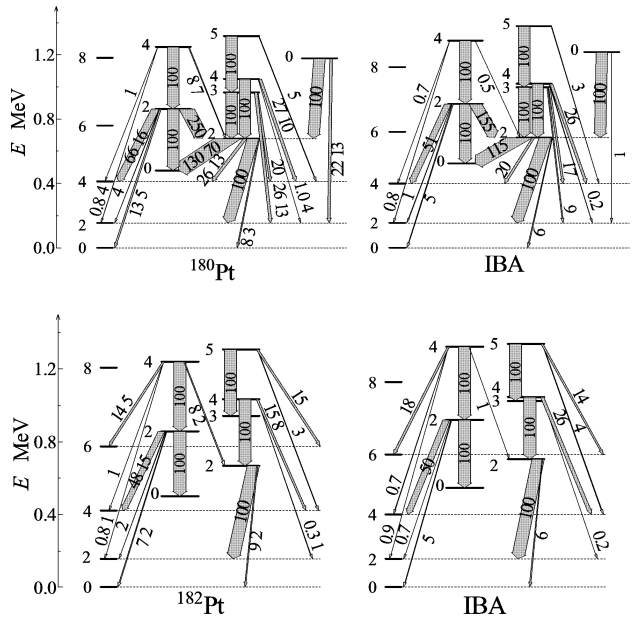

FIGURE 6. Comparison of experimental (left) and IBA calculations (right) for energy levels and electromagnetic transition strengths in ^{180}Pt (top) and ^{182}Pt (bottom). The thickness of the arrow indicates the relative $B(E2)$ strengths which are also labelled by their values.

A more detailed look into the quality of the fits is presented in Fig. 6 for ^{180}Pt and ^{182}Pt. For both of these nuclei, the calculations show a remarkable level of agreement with the experimental data. The energy spacings in the ground state band and the excited 0^+ sequence along with the staggering in the γ band are well reproduced. The quality of the predictions for the spacing in the excited 0^+ sequence are somewhat interesting since the IBA fails to reproduce this observable in the transitional and rotational rare-earth nuclei as discussed above. The reason for the lack of agreement in the rare-earth nuclei or the success of the predictions in the Pt nuclei remains an open question. The calculations for branching ratios from excited states in the excited 0^+ sequence and the γ band are in near perfect agreement with the experimental data.

In conclusion, motivated by the ability of the X(5) model to describe certain rare-earth nuclei with parameter free predictions, a reinvestigation into the evolution of structure in the rare-earth region using two parameter (plus scaling) IBA-1 calculations was performed. First, contours of basic observables were discussed in the IBA triangle and a simple set of quasi-orthogonal contours was identified for determining parameter values. Using this approach, a good description of all positive parity low-lying excitations in the Gd-Os isotopes was obtained and the resulting parameters were mapped into the IBA symmetry triangle. These calculations were extended to the Pt isotopic chain, obtaining excellent agreement for both energies and electromagnetic transition strengths. The ability of the IBA to reproduce the structure of the Pt isotopes with a single space Hamiltonian illustrates that the Pt isotopes can be well described without the introduction of intruder state configurations.

Acknowledgments

These results stem from collaborations with R.F. Casten and N.V. Zamfir, whom I thank for their valuable discussions and input. This work is supported by the U.S. DOE Grant No. DE-FG02-91ER-40609.

1. F. Iachello, *Phys. Rev. Lett.* **87** (2001) 052502.
2. R.F. Casten and N.V. Zamfir, *Phys. Rev. Lett.* **87** (2001) 052503.
3. R. Krücken *et al.*, *Phys. Rev. Lett.* **88** (2002) 232501.
4. D. Tonev *et al.*, *Phys. Rev. C* **69** (2004) 034334.
5. M.A. Caprio *et al.*, *Phys. Rev. C* **66** (2002) 054310.
6. F. Iachello and A. Arima, *The Interacting Boson Model* (Cambridge University Press, Cambridge, 1987).
7. W.-T. Chou, N.V. Zamfir, and R.F. Casten, *Phys. Rev. C* **56** (1997) 829.
8. P.O. Lipas, P. Toivonen, and D.D. Warner, *Phys. Lett. B* **155** (1985) 295.
9. V. Werner, N. Pietralla, P. von Brentano, R.F. Casten, and R.V. Jolos, *Phys. Rev. C* **61** (2000) 021301(R).
10. N.V. Zamfir, P. von Brentano, R.F. Casten, and J. Jolie, *Phys. Rev. C* **66** (2002) 021304(R).
11. R.F. Casten and D.D. Warner, in *Progress in Particle and Nuclear Physics*, edited by D. Wilkinson (Pergamon, Oxford, 1983) Vol. 9, p. 311.
12. E.A. McCutchan, N.V. Zamfir, and R.F. Casten, Phys. Rev. C **69** (2004) 064306.
13. D.D. Warner and R.F. Casten, *Phys. Rev. Lett.* **48**, 1385 (1982).
14. D. Bucurescu *et al.*, *Z. Phys. A* **324** (1986) 387.
15. E.A. McCutchan and N.V. Zamfir, *Phys. Rev. C* **71** (2005) 054306.
16. J.L. Wood, K. Heyde, W. Nazarewicz, M. Huyse, and P. van Duppen, *Phys. Rep.* **215** (1992) 101.
17. R. Julin, K. Helariutta, and M. Muikku, *J. Phys. G: Nucl. Part. Phys.* **27** (2001) 109(R).
18. P.M. Davidson *et al.*, *Nucl. Phys. A* **657** (1999) 219.
19. M.K. Harder, K.T. Tang, and P. Van Isacker, *Phys. Lett. B* **405** (1997) 25.
20. E.A. McCutchan, R.F. Casten, and N.V. Zamfir, *Phys. Rev. C* **71** (2005) 061301(R).